nature communications

Article

https://doi.org/10.1038/s41467-024-55809-3

Variation in a single allele drives divergent yield responses to elevated CO_2 between rice subspecies

Received: 21 August 2024

Accepted: 30 December 2024

Published online: 03 January 2025

Check for updates

Yunlong Liu[1,2,3,10], Siyu Zhang[1,2,10], Haoyu Qian[2,3], Chengbo Shen[1,2], Shuijin Hu[4], Weijian Zhang[5], Yong Wang[6], Shan Huang[6], Songhan Wang[2,3], Zhenghui Liu[2,3], Ganghua Li[2,3], Xiangdong Fu[7,8], Yanfeng Ding[1,2,3] ✉, Shan Li[1,2] ✉, Kees Jan van Groenigen[9] & Yu Jiang[1,2,3] ✉

Rising atmospheric CO_2 generally increases yield of *indica* rice, one of the two main Asian cultivated rice subspecies, more strongly than *japonica* rice, the other main subspecies. The molecular mechanisms driving this difference remain unclear, limiting the potential of future rice yield increases through breeding efforts. Here, we show that between-species variation in the *DNR1* (*DULL NITROGEN RESPONSE1*) allele, a regulator of nitrate-use efficiency in rice plants, explains the divergent response to elevated atmospheric CO_2 (eCO_2) conditions. eCO_2 increased rice yield by 22.8–32.3% in plants carrying or mimicking the *indica DNR1* allele, but only by 3.6–11.1% in plants carrying the *japonica DNR1* allele. Rice plants carrying or mimicking the *indica DNR1* allele exhibit decreased eCO_2-responsive transcription and protein abundance of DNR1, which activates genes involved in nitrate transport and assimilation, driving the increase in plant growth. Our findings identify the *indica DNR1* gene as a key breeding resource for sustainably enhancing nitrate uptake and rice yields in *japonica* varieties, potentially contributing to global food security as atmospheric CO_2 levels continue to increase.

Atmospheric CO_2 concentrations have increased from 315 ppm in 1958 to 423 ppm in 2024 and are expected to further increase to 800 ppm by the end of the 21st century due to human activities such as fossil fuel consumption and deforestation[1,2]. Elevated CO_2 concentration (eCO_2) often stimulates photosynthesis and yields of C3 plants[3–5], also known as the CO_2 fertilization effect. Global meta-analyses of free air CO_2 enrichment (FACE) experiments showed that eCO_2 increased photosynthesis by 22% and yield by 14% in rice[4,6]. Rice sustains approximately half of the global population and provides about one-fifth of the world's dietary energy supply[7]. Furthermore, global rice yields are predicted to reduce due to global climate warming[8,9]. In this context, the role of atmospheric changes, particularly the increase in CO_2 levels, becomes a pivotal factor in understanding future trends in rice production and global food security.

Around 90% of rice cultivation occurs in Asia, where two major subspecies, *indica* (Xian) and *japonica* (Geng), each with distinct

[1]State Key Laboratory of Crop Genetics & Germplasm Enhancement and Utilization, Nanjing Agricultural University, Nanjing, China. [2]Jiangsu Collaborative Innovation Center for Modern Crop Production, Nanjing Agricultural University, Nanjing, China. [3]Key Laboratory of Crop Physiology and Ecology in Southern China, Nanjing Agricultural University, Nanjing, China. [4]Department of Entomology & Plant Pathology, North Carolina State University, Raleigh, NC, USA. [5]Institute of Crop Sciences, Chinese Academy of Agricultural Sciences, Beijing, China. [6]Ministry of Education and Jiangxi Key Laboratory of Crop Physiology, Ecology and Genetic Breeding, Jiangxi Agricultural University, Nanchang, China. [7]State Key Laboratory of Plant Cell and Chromosome Engineering, Institute of Genetics and Developmental Biology, Innovation Academy for Seed Design, Chinese Academy of Sciences, Beijing, China. [8]College of Life Sciences, University of Chinese Academy of Sciences, Beijing, China. [9]Department of Geography, Faculty of Environment, Science and Economy, University of Exeter, Exeter, UK. [10]These authors contributed equally: Yunlong Liu, Siyu Zhang. ✉e-mail: dingyf@njau.edu.cn; shanli@njau.edu.cn; yujiang@njau.edu.cn

developmental and physiological traits, are cultivated[10]. *Japonica* rice, domesticated in the Yangtze River basin around 9000 to 6000 years ago, is predominantly grown and consumed in East Asia, comprising about 40% of the rice cultivation area in China, Japan, and Korea[11]. In contrast, *indica* rice, first domesticated in the Ganges region between 8500 and 4500 years ago, is more prevalent in most other regions. However, CO_2 fertilization effect varies between *indica* and *japonica*[6,12–14], with *indica* varieties showing a more pronounced increase in yield (+20.4%) under eCO_2 conditions compared to *japonica* varieties (+12.7%)[12]. The disparity in the CO_2 fertilization between subspecies may strongly affect future global total rice yields; the difference between all rice globally responding to eCO_2 like *japonica* or like *indica* amounts to ~109 Tg per year, equal to roughly half of China's annual rice production. However, the underlying mechanisms driving this divergence in response to eCO_2 between rice subspecies, especially at the molecular level, remain largely unexplored.

Nitrogen (N) is a critical nutrient for plant growth, and its availability and uptake significantly affect the response of C3 plants, including rice, to eCO_2 conditions[3,15,16]. In rice, nitrate (NO_3^-) and ammonium (NH_4^+) serve as the primary inorganic N sources[17]. Due to nitrification in the rhizosphere, up to 40% of the total N absorbed and utilized by rice is NO_3^-[18]. Notably, *indica* rice varieties generally exhibit higher capacities of both NO_3^- uptake and assimilation compared to *japonica*, whereas the two subspecies show similar NH_4^+ uptake rates[19,20]. Consistent with these results, we found that *japonica* varieties exhibited significantly lower NO_3^- uptake rates that were less sensitive to changes in external CO_2 status compared with *indica* varieties (Supplementary Fig. 1). Furthermore, we observed an interactive effect on NO_3^- uptake ($P = 0.001$), but not on NH_4^+ absorption ($P = 0.373$), between eCO_2 and rice species. The NO_3^- uptake rates in *japonica* varieties were less responsive to eCO_2 (+40%) compared to *indica* varieties (+69%) (Supplementary Fig. 1). Based on these observations, we hypothesize that variations in NO_3^--use efficiency might contribute to the divergent yield responses to eCO_2 between *indica* and *japonica*.

Recent studies have identified five genes-*OsNRT1.1B*, *OsNR2*, *DULL NITROGEN RESPONSE1* (*DNR1*), *REGULATOR OF N-RESPONSIVE RSA ON CHROMOSOME 10* (*RNR10*), and *MYB61*-that are involved in NO_3^- use efficiency and that exhibit allelic variations between *indica* and *japonica* rice subspecies[19,21–24] (Supplementary Tables 1, 2). To evaluate the response of genetic variations to eCO_2, we performed an RNA-seq analysis, using the flag leaves of a typical *indica* variety Yangdao 6 (YD6) and a typical *japonica* variety Zhonghua 11 (ZH11) at the heading stage in a FACE experiment (See supplementary method). We found that while eCO_2 (~ +150 ppm) decreased *DNR1* abundance in the leaves of YD6, it did not significantly affect its expression in ZH11 (Supplementary Fig. 2a). In contrast, the responses of the other four genes to eCO_2 were similar between the two varieties (Supplementary Fig. 2b–e). Furthermore, we found that the *DNR1* allele varies between *japonica* and *indica* varieties frequently used in FACE experiments (Supplementary Table 3). Notably, rice varieties with the *indica DNR1* allele were more responsive to eCO_2 (Supplementary Fig. 3).

DNR1, a negative regulator of auxin biosynthesis, has diverged in sequence between the two rice subspecies[23]. Plants carrying the *indica DNR1* variant confers reduced DNR1 mRNA and protein abundance and subsequently increased auxin accumulation, thereby inducing transcriptional activation of genes coding NO_3^- uptake and downstream NO_3^- assimilation enzymes (Supplementary Fig. 4, Supplementary Table 2), leading to high N-use efficiency (NUE) and grain yield[23]. As expected, eCO_2 increased the rice biomass, N uptake and yields more strongly in YD6 than those in ZH11 (Supplementary Fig. 5). These findings suggest that *DNR1* variations could play a significant role in the divergent rice responses to eCO_2 between rice subspecies.

Results

DNR1 variation drives divergent yield responses to elevated CO_2

To evaluate whether the *DNR1* variation contributes to the divergent responses to eCO_2 between rice subspecies, we carried out a field experiment within a FACE system to compare typical *japonica* variety ZH11 and its *dnr1* mutants, which mimics the *indica DNR1* allele against a ZH11 background by reducing DNR1 abundance[23]. eCO_2 reduced both *DNR1* transcript and protein abundances in ZH11, and DNR1 protein levels were undetectable in the *dnr1* mutants under both eCO_2 and aCO_2 conditions, due to the complete loss-of-function nature of the *DNR1* variant (Fig. 1a, b). We found that eCO_2 stimulated the growth of the *dnr1* mutants more strongly than the ZH11 variety (Fig. 1c). At the heading stage, eCO_2 increased the light-saturated net photosynthesis rate more strongly in *dnr1* mutants than in ZH11 (Supplementary Fig. 6a). eCO_2 significantly reduced stomatal conductance (g_s), maximum rate of RuBP carboxylation (*Vcmax*), maximum rate of electron transport driving RuBP regeneration (*J max*), and non-photochemical quenching (NPQ) (Supplementary Figs. 6, 7). While *dnr1* mutants exhibited higher *Vcmax* and NPQ compared to ZH11, eCO_2 had no effect on the quantum yield of Photosystem II (Y(II)), the photochemical quenching coefficient (qL), or the maximum photochemical quantum yield of PSII (Fv/Fm) (Supplementary Fig. 7). eCO_2 increased leaf area by 40.8% in *dnr1* mutants, compared to only 6.6% increases in ZH11 (Supplementary Fig. 8a). In agreement with previous studies[6], eCO_2 tended to reduce the N content of flag leaf due to the dilution effect (Supplementary Fig. 8b). eCO_2 increased N uptake more substantially in *dnr1* mutants than in ZH11 (Supplementary Fig. 8c).

At maturity stage, the aboveground biomass, N uptake, and rice yield were all significantly higher in the *dnr1* mutants compared to ZH11 (Fig. 1c–e). The impacts of eCO_2 on these parameters were clearly dependent on the *DNR1* allele. In *dnr1* mutants, eCO_2 stimulated the aboveground biomass, N uptake, and rice yield by 17.8%, 17.8%, and 22.8%, respectively, while it had no significant effects on ZH11 (Fig. 1c–e). Also, eCO_2 stimulated N-use efficiency (NUE) more strongly in *dnr1* than in ZH11 (Fig. 1f).

To test whether *DNR1* variation also causes differential responses to eCO_2 within an *indica* variety, we compared the effects of eCO_2 on the typical *indica* variety, Hua-Jing-Xian 74 (HJX74), with a near-isogenic line (NIL) carrying the *japonica DNR1* allele for two years. The *indica* HJX74 exhibited lower *DNR1* transcripts and protein abundance compared to NIL, and the changes induced by eCO_2 were stronger in HJX74 (Supplementary Fig. 9a, b). More importantly, eCO_2 stimulated rice plant growth parameters (i.e., photosynthesis rate, leaf area, biomass, N uptake, and NUE) more strongly in HJX74 than in NIL (Supplementary Figs. 9, 10). At maturity, eCO_2 significantly increased rice yield by 27.6–32.3% in HJX74, but only by 3.6–11.1% in NIL (Supplementary Figs. 9j, 10h). Taken together, our findings indicate that the variation in the *DNR1* allele plays a crucial role in driving the divergent responses to eCO_2 between rice subspecies.

DNR1 variation affects response of N metabolism to eCO_2

To determine how *DNR1* variation affects the response of N metabolism to eCO_2, we conducted a 14-day hydroponic experiment in walk-in growth chambers, administering either aCO_2 or eCO_2 treatments to ZH11 and *dnr1* mutants, as well as HJX74 and NIL. Similar with results of FACE experiment, eCO_2 enhanced aboveground biomass, especially in *dnr1* mutants (Fig. 2a, c). eCO_2 also enlarged root system architecture (RSA), including total root length, total area, and the total number of root tips (Fig. 2b, d–f). While eCO_2 increased $^{15}NO_3^-$ uptake rates in both ZH11 and *dnr1* mutants (Fig. 2g), the positive effect of eCO_2 was more pronounced in the *dnr1* mutants (Fig. 2). Similarly, eCO_2 promotes aboveground biomass, RSA and $^{15}NO_3^-$ absorption rate more strongly in HJX74 than in NIL (Supplementary Fig. 11a–g). These effects are attributed to increased IAA content under eCO_2 treatment, caused

https://doi.org/10.1038/s41467-024-55809-3

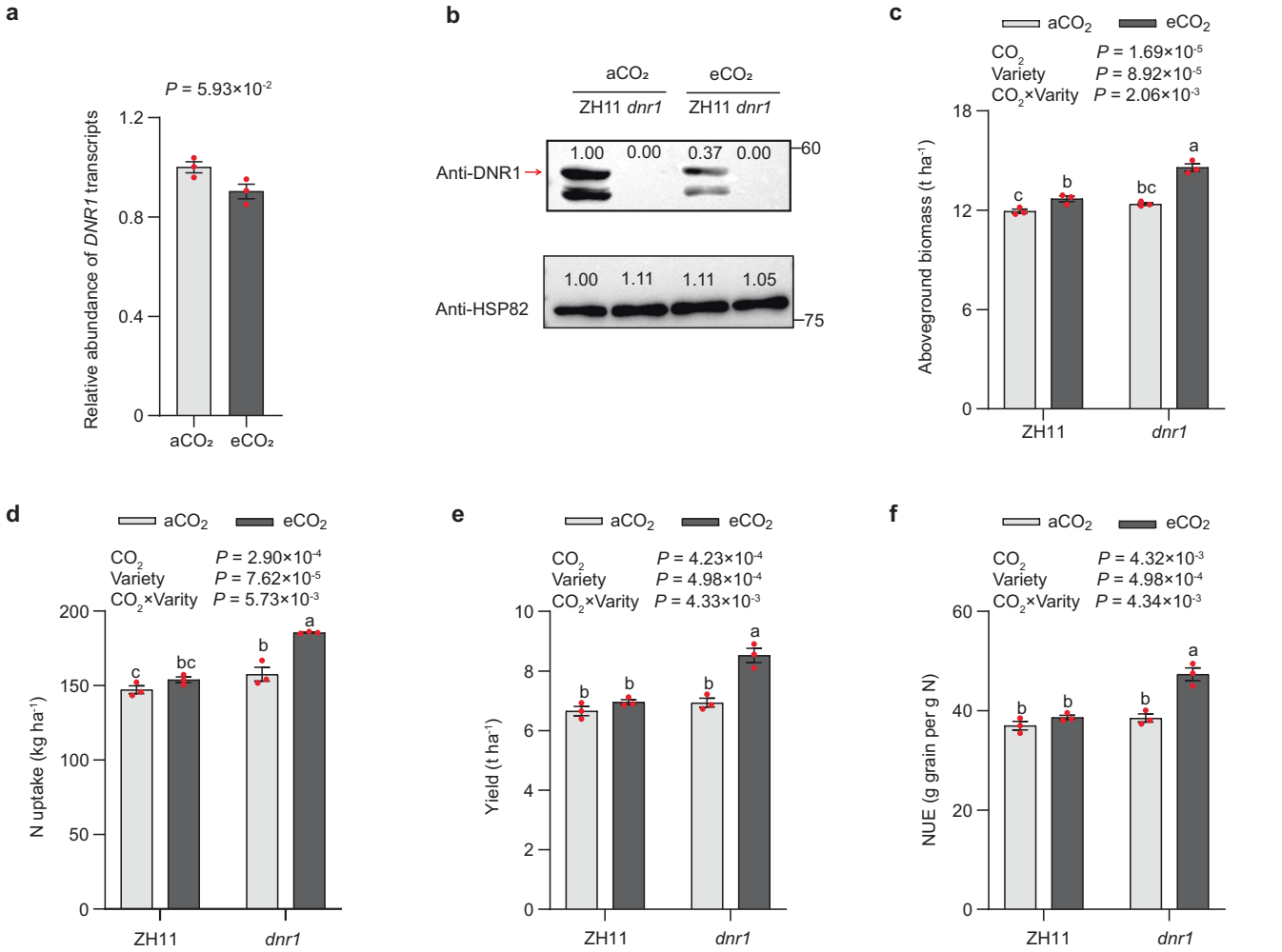

Fig. 1 | Different responses of *japonica* variety Zhonghua 11 (ZH11) and its *dnr1* mutants mimicking the *indica DNR1* allele to elevated CO_2. **a** *DNR1* transcript abundance in ZH11 shoots under ambient CO_2 (aCO_2) and elevated CO_2 (eCO_2) conditions. Transcript abundance was measured relative to ZH11 under aCO_2 (set to 1). Data are mean ± s.e.m. ($n = 3$ biological replicates). *P*-value was generated from two-sided Student's *t* tests. **b** DNR1 protein abundance in the shoots of ZH11 and *dnr1* under aCO_2 and eCO_2 conditions. HSP82 serves as a loading control. The red arrow indicates the DNR1 bands. Data are representative of three independent experiments, with similar results. Aboveground biomass (**c**), N uptake (**d**), yield (**e**) and N-use efficiency (**f**) under aCO_2 and eCO_2 conditions were measured at maturity. ZH11 and *dnr1* indicate *japonica* variety Zhonghua 11 and its *dnr1* mutants, respectively. **c**–**f** Data are mean ± s.e.m. ($n = 3$ biological replicates). *P*-values were generated from two-way ANOVA. Different letters indicate significant differences among treatments ($P < 0.05$). Source data are provided as a Source Data file.

by the inhibition of DNR1 expression, particularly in the *dnr1* mutant and HJX74 (Fig. 2h; Supplementary Fig. 11h).

Additionally, we conducted hydroponic experiments using either NO_3^- (KNO_3) or NH_4^+ ($(NH_4)_2SO_4$) as the N source for ZH11 and *dnr1* plants. *dnr1* plants consistently showed a higher responsiveness to variable CO_2 levels in both NO_3^- and NH_4^+ conditions compared to ZH11 (Supplementary Fig. 12). However, the responses of aboveground and root biomass in both ZH11 and *dnr1* were more pronounced under eCO_2 when NO_3^- was provided, compared to NH_4^+ (Supplementary Fig. 12). Therefore, it is reasonable to conclude that DNR1 plays a crucial role in mediating plant growth in response to varying CO_2 levels, particularly with NO_3^-.

DNR1 acts as an antagonist to auxin biosynthesis, triggering AUXIN RESPONSE FACTORs (OsARF6 and OsARF17)-mediated activation of genes associated with NO_3^- uptake and metabolism, thereby contributing to enhanced NUE and grain yield[23] (Supplementary Fig. 1). To determine whether eCO_2 influences NO_3^- metabolism by modulating DNR1-mediated auxin homeostasis, we conducted RT-qPCR analysis of key genes involved in the DNR1-auxin-N pathway, including *OsARF6*, *OsARF17*, *OsNRT1.1B*, *OsNRT2.3a*, *OsNPF2.4*, and *OsNIA2*. As anticipated, eCO_2 significantly increased transcription levels of *OsARF6*, *OsARF17*, *OsNRT1.1B*, *OsNRT2.3a*, *OsNPF2.4*, and *OsNIA2* (Figs. 2h and 3a–f). Correspondingly, nitrate reductase (NR) activity was markedly enhanced under eCO_2 conditions (Supplementary Fig. 13a). Notably, eCO_2 stimulated the expression of these genes in the *dnr1* mutants more strongly than in ZH11, resulting in higher NO_3^- uptake rate and NR activity (Fig. 3; Supplementary Fig. 13a). Similar trends were observed in HJX74 and NIL, with or without eCO_2 treatment (Supplementary Figs. 13b and 14).

Next, we investigated whether eCO_2 could stimulate NO_3^- uptake and assimilation through the involvement of OsARFs, which act as downstream transcription factors of auxin homeostasis mediated by DNR1. Firstly, we conducted a time course assessment of the expression levels of *OsARF6*, *OsARF17*, *OsNRT1.1B*, *OsNRT2.3a*, *OsNPF2.4*, and *OsNIA2* and found that the expression patterns of these four N-related genes and *OsARFs* are aligned. Specifically, when *OsARFs* expression is strongly induced by eCO_2 (30 min to 2 h), the expression of *OsNRT1.1B*, *OsNRT2.3a*, *OsNPF2.4*, and *OsNIA2* also significantly increases, suggesting that OsARFs regulates these genes in response to eCO_2 (Supplementary Fig. 15). Interestingly, under eCO_2 conditions, *OsNRT1.1B* shows a quicker response, which may be due to its direct response to CO_2 concentration changes.

https://doi.org/10.1038/s41467-024-55809-3

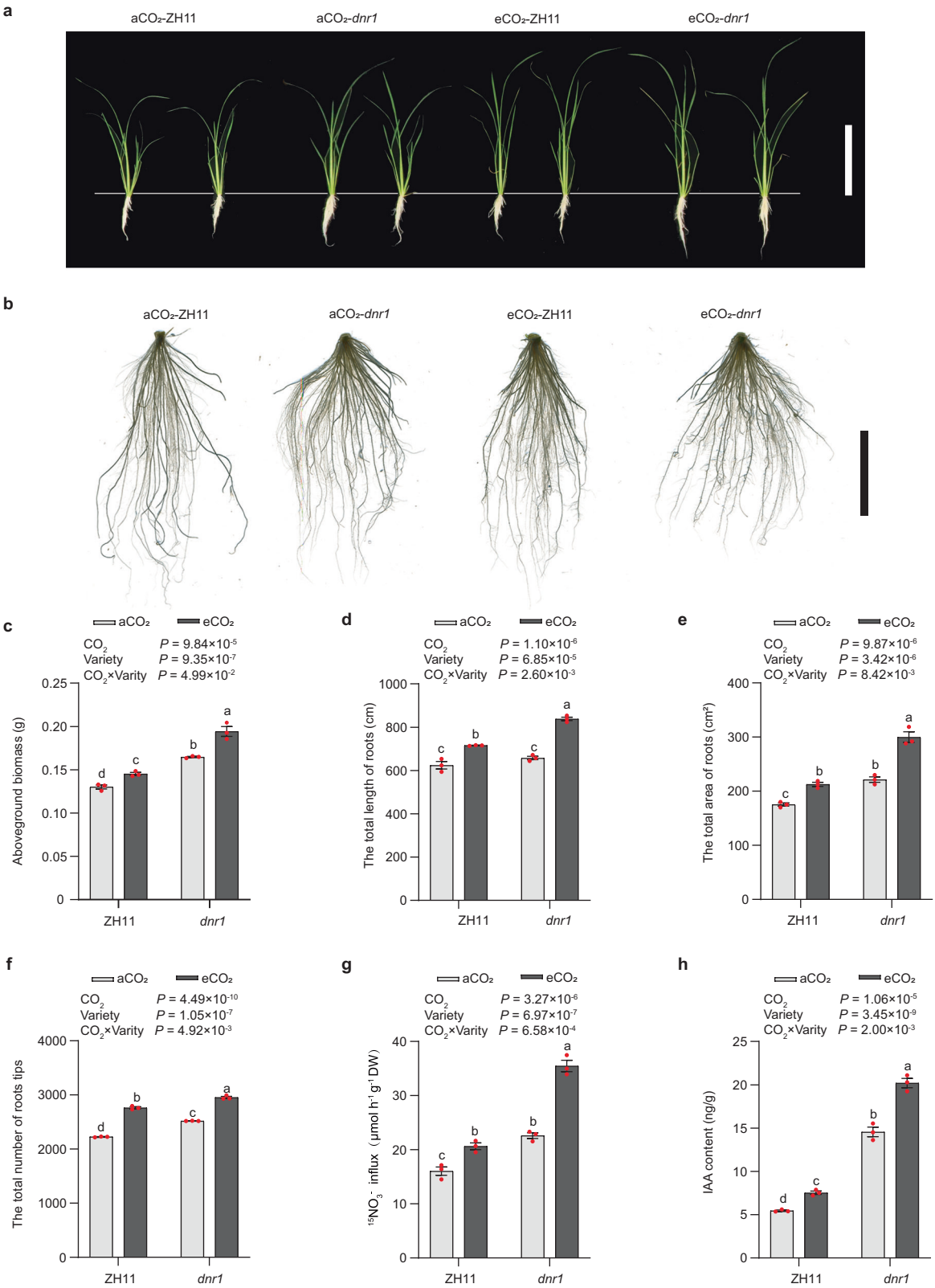

Fig. 2 | Differences in plant growth and root developmental plasticity in response to elevated CO_2 between *japonica* variety Zhonghua 11 (ZH11) and its *dnr1* mutants mimicking the *indica DNR1* allele. a, **b** 14-day-old *japonica* variety Zhonghua 11 (ZH11) and its *dnr1* mutants (*dnr1*) rice plants grown under ambient CO_2 (aCO_2) and elevated CO_2 (eCO_2) conditions, respectively. Morphology of plants (**a**) and root systems (**b**). **a** Scale bar, 20 cm. **b** Scale bar, 5 cm. **c** Aboveground biomass. Root statistics of total length of visible roots (**d**), total area of visible roots (**e**), and number of root tips (**f**). $^{15}NO_3^-$ uptake rates (**g**) and root free IAA content (**h**) of *japonica* variety ZH11 and *dnr1* under aCO_2 and eCO_2 conditions. **c**–**h** Data are mean ± s.e.m. ($n = 3$ biological replicates). *P*-values were generated from two-way ANOVA. Different letters indicate significant differences among treatments ($P < 0.05$). Source data are provided as a Source Data file.

https://doi.org/10.1038/s41467-024-55809-3

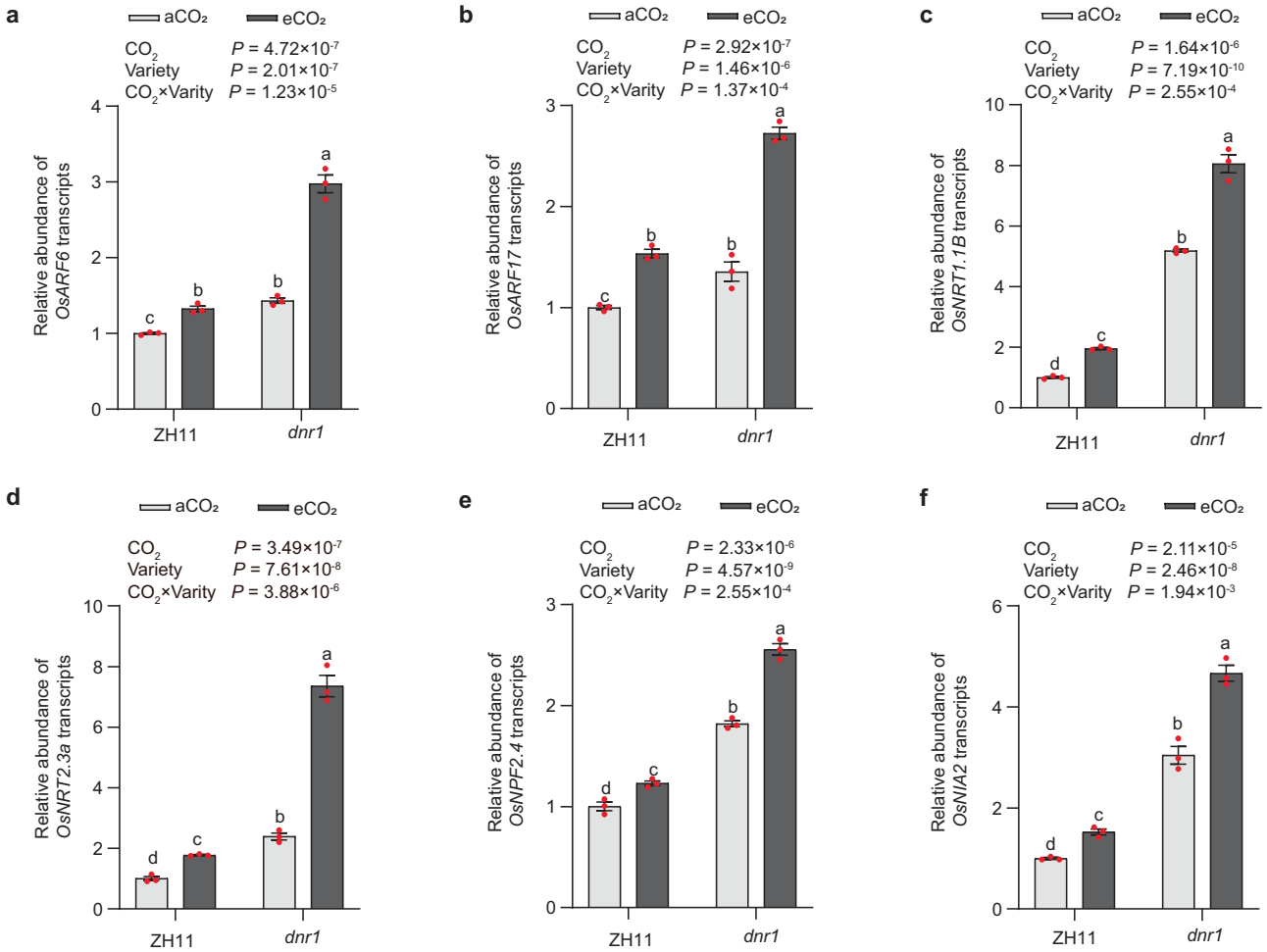

Fig. 3 | Elevated CO_2 enhances NO_3^- metabolism via DNR1-mediated auxin homeostasis in *japonica* variety Zhonghua 11 (ZH11) and its *dnr1* mutants mimicking the *indica DNR1* allele. Root mRNA abundances of *OsARF6* (**a**) and *OsARF17* (**b**) grown under ambient CO_2 (aCO_2) and elevated CO_2 (eCO_2) conditions, relative to ZH11 under aCO_2 (set to 1). Root mRNA abundances of *OsNRT1.1B* (**c**) and *OsNRT2.3a* (**d**) relative to ZH11 under aCO_2 (set to 1). Shoot mRNA abundances of *OsNPF2.4* (**e**) and *OsNIA2* (**f**) relative to ZH11 under aCO_2 (set to 1). ZH11 and *dnr1* indicate *japonica* variety Zhonghua 11 and its *dnr1* mutants, respectively. **a**–**f** Data are mean ± s.e.m. ($n = 3$ biological replicates). *P*-values were generated from two-way ANOVA. Different letters indicate significant differences among treatments ($P < 0.05$). Source data are provided as a Source Data file.

To test this hypothesis, we used HJX74 and a single-segment substitution line (SSSL-064), generated by crossing IRAT261 (donor parent) with HJX74 (recurrent parent), which incorporates a chromosome segment containing *OsNRT1.1B* from *japonica* IRAT261 into the HJX74 genetic background to investigate the response of *OsNRT1.1B* to eCO_2. Both HJX74 and SSSL-064 exhibited increased biomass and $^{15}NO_3^-$ uptake under eCO_2 compared to aCO_2, with HJX74 showing a slightly more pronounced increase (Supplementary Fig. 16). These results indicate that *OsNRT1.1B* itself can influence $^{15}NO_3^-$ absorption and thereby affect growth to some extent in response to eCO_2.

Secondly, to further illustrate the regulatory effects of OsARF6 and OsARF17 under aCO_2 and eCO_2 conditions, we performed ChIP-qPCR assays. These assays indicated that eCO_2 enhanced the enrichment of TGTCTC/GAGACA motif-containing fragments from the promoters of *OsNRT1.1B*, *OsNRT2.3a*, *OsNPF2.4*, and *OsNIA2* compared to the aCO_2 treatment (Fig. 4a–d; Supplementary Fig. 17a–f). The following in vitro transient transactivation assays revealed that eCO_2 increased the transcriptional activation capacities of OsARF6 and OsARF17 towards their downstream genes, *OsNRT1.1B*, *OsNRT2.3a*, *OsNPF2.4*, and *OsNIA2*, when compared to aCO_2 treatment (Fig. 4e, f; Supplementary Fig. 17g, h). Accordingly, under both aCO_2 and eCO_2 conditions, the expression levels of *OsNRT1.1B*, *OsNRT2.3a*, *OsNPF2.4*, and *OsNIA2* were upregulated in the *OsARF6* or *OsARF17* overexpression lines within the ZH11/*pACT::DNR1-Flag* background (Fig. 4g–j). These results further confirm the transactivation activities of OsARFs towards N-related genes in rice protoplasts (Fig. 4e, f; Supplementary Fig. 17g, h).

Finally, we tested whether the altered transcriptional activation capacities of OsARF6 and OsARF17 led to changes in NO_3^- uptake in response to eCO_2. Under eCO_2, the over-expression of *OsARF6* or *OsARF17* in the ZH11/*pACT::DNR1-Flag* background significantly restored the insensitivities of NO_3^- absorption caused by auxin depletion (Fig. 4k). This suggests that eCO_2 promotes NO_3^- uptake and assimilation by enhancing the transcriptional activation capacities of OsARFs.

DNR1 variation affects response of photosynthetic genes to eCO_2

As a crucial substrate for photosynthesis, CO_2 actively participates in the photosynthetic processes of plants. Thus, we compared the transcription and protein levels of core elements in photosystems (*OsPsbA*, *OsPsaB*), and rate-limiting factors in the Calvin-Benson cycle (*OsRbcs*, *OsRbcL* and *OsSBPase*) (Supplementary Table 4), in both ZH11 and *dnr1* mutants with or without CO_2 treatment. Both transcription and protein levels of *OsPsaB*, *OsRbcS* and *OsSBPase* were significantly higher in *dnr1* mutants compared to ZH11, and the changes induced by eCO_2 were

https://doi.org/10.1038/s41467-024-55809-3

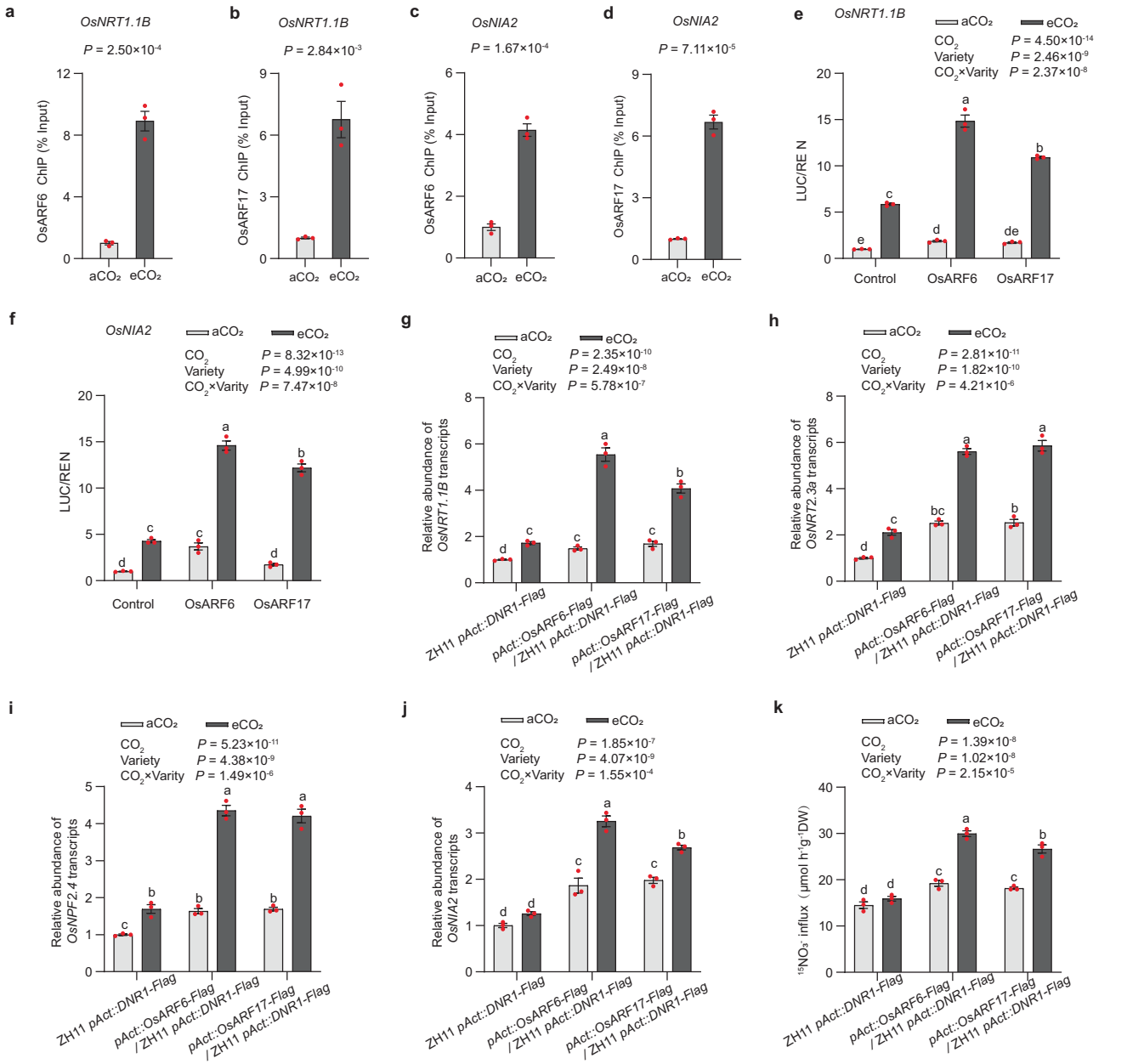

Fig. 4 | The effect of elevated CO_2 on the expression of N metabolism-related genes and NO_3^- uptake is mediated by DNR1-OsARFs module. Extent of OsARF6 and OsARF17-mediated ChIP-qPCR enrichment (relative to Input) of TGTCTC-containing promoter fragments from OsNRT1.1B (**a**, **b**) and OsNIA2 (**c**, **d**) under ambient CO_2 (aCO_2) and elevated CO_2 (eCO_2) conditions. Data are mean ± s.e.m. ($n = 3$ biological replicates). *P*-values were generated from two-sided Student's *t* tests. OsARF6 and OsARF17 activate *OsNRT1.1B* (**e**) and *OsNIA2* (**f**) promoter-LUC fusion constructs in transient transactivation assays. The LUC/REN activity obtained from a co-transfection with an empty effector construct and indicated reporter constructs under ambient CO_2 (aCO_2) was set to 1. Root mRNA abundances of *OsNRT1.1B* (**g**) and *OsNRT2.3a* (**h**) relative to ZH11 *pAct::DNR1-Flag* under aCO_2 (set to 1). **i**, **j** Shoot mRNA abundances of *OsNPF2.4* (**i**) and *OsNIA2* (**g**) relative to ZH11 *pAct::DNR1-Flag* under aCO_2 (set to 1). **k** Root $^{15}NO_3^-$ uptake rate of *OsARF6* and *OsARF17* overexpression lines in the ZH11 *pAct::DNR1-Flag* background grown under aCO_2 and elevated CO_2 (eCO_2) conditions, respectively. **e**–**k** Data are mean ± s.e.m. ($n = 3$ biological replicates). *P*-values were generated from two-way ANOVA. Different letters indicate significant differences among treatments ($P < 0.05$). Source data are provided as a Source Data file.

more pronounced in *dnr1* mutants (Fig. 5). However, although the expression levels of *OsPsbA*, *OsRbcS4* and *OsRbcL* slightly increased in *dnr1*, they appear to be unaffected by eCO_2 (Supplementary Fig. 18). Similar results were found for HJX74 and NIL (Supplementary Fig. 19), confirming that the abundance patterns of photosynthetic genes induced by eCO_2 in ZH11 and *dnr1* mutants were shared by these varieties.

We found that OsARF6 and OsARF17 do not possess transcriptional activation abilities for these genes under both aCO_2 and eCO_2 conditions (Supplementary Fig. 20a), suggesting that eCO_2 promotes the accumulation of photosynthesis-related proteins and enhances photosynthesis independent on OsARFs. Additionally, examining the expression levels of these genes in plants overexpressing *OsARF6* and *OsARF17* within the ZH11/*pACT::DNR1-Flag* background revealed no changes compared to ZH11/*pACT::DNR1-Flag* with either aCO_2 or eCO_2 treatment (Supplementary Fig. 20b–g). This suggests that DNR1 does not regulate photosynthetic efficiency through the transcriptional activation of OsARF6 and OsARF17.

We conducted RNA sequencing analysis on ZH11 and the *dnr1* mutant under both aCO_2 and eCO_2 conditions and identified 397 target

https://doi.org/10.1038/s41467-024-55809-3

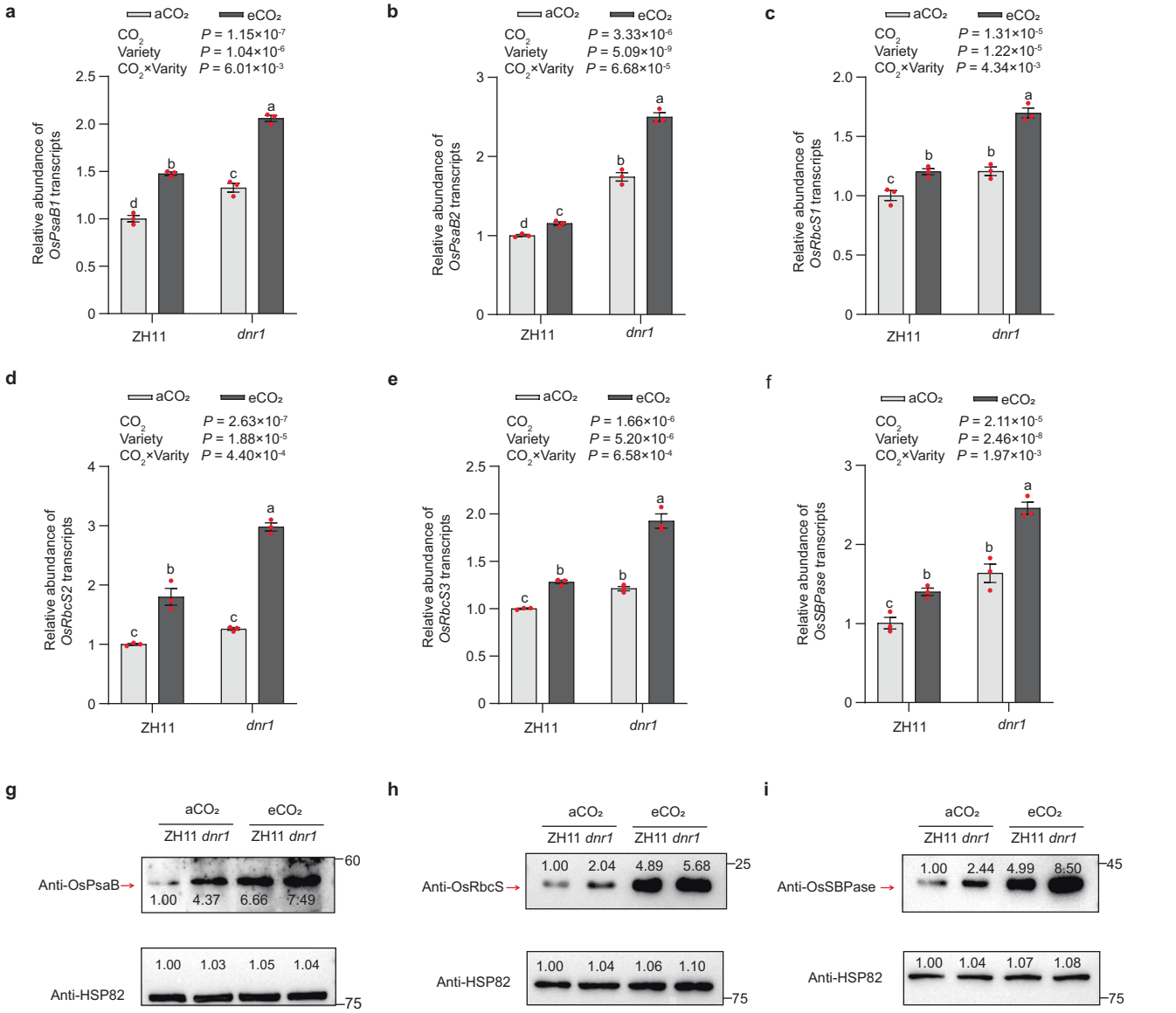

Fig. 5 | The impact of elevated CO_2 on DNR1-regulated abundances of photosynthetic genes in *japonica* variety Zhonghua 11 (ZH11) and its *dnr1* mutants mimicking the *indica DNR1* allele. Shoot mRNA abundances of *OsPsaB1* (**a**), *OsPsaB2* (**b**), *OsRbcS1* (**c**), *OsRbcS2* (**d**), *OsRbcS3* (**e**), and *OsSBPase* (**f**) grown ambient CO_2 (aCO_2) and elevated CO_2 (eCO_2) conditions, respectively, relative to Zhonghua 11 under aCO_2 (set to 1). Data are mean ± s.e.m. ($n = 3$ biological replicates). *P*-values were generated from two-way ANOVA. Different letters indicate significant differences among treatments ($P < 0.05$). OsPsaB (**g**), OsRbcS (**h**) and OsSBPase (**i**) protein abundances in shoots. HSP82 serves as a loading control. The red arrows indicate the OsPsaB, OsRbcS and OsSBPase bands, respectively. Data are representative of three independent experiments, with similar results. Source data are provided as a Source Data file.

genes regulated by both CO_2 and DNR1. Among these, 9 transcription factors are upregulated by both eCO_2 and null-*DNR1* allele, and 4 transcription factors are downregulated by both eCO_2 and null-*DNR1* allele (Supplementary Table 5). These 13 transcription factors may serve as potential candidates for regulating photosynthetic efficiency in response to eCO_2 and DNR1 interactions, offering promising avenues for future research. Overall, eCO_2 enhances photosynthetic efficiency by improving the C and N cycles through various mechanisms.

Discussion

We present evidence of the key role of DNR1 in driving the divergent responses of *indica* and *japonica* rice varieties to eCO_2 (Fig. 6). eCO_2 likely influences DNR1 indirectly through changes in N status. eCO_2 can increase photosynthesis and plant growth, thereby raising the demand for nitrogen. This, in turn, could lead to a decrease in DNR1 abundance, stimulating N uptake. Specifically, plants carrying the *japonica DNR1* allele, which exhibit higher DNR1 abundance leading to reduced auxin accumulation, key traits such as biomass, nitrogen content, and yield respond relatively weakly to eCO_2. Conversely, in *dnr1* mutants, eCO_2 decreases the expression of DNR1 and the following transcriptional activation of OsARF6 and OsARF17, which in turn upregulates genes associated with NO_3^- uptake and assimilation (*OsNRT1.1B*, *OsNRT2.3a*, *OsNIA2*, and *OsNPF2.4*). Consequently, N uptake and assimilation increased, resulting in elevated N content in rice plants, which enhanced the photosynthetic capacity of the plants under eCO_2 concentrations. Additionally, previous studies have shown that IAA levels rise under eCO_2[25–27]. Our results suggest that the inhibition of DNR1 by eCO_2 may also contribute to this increase in IAA content, which further enhances our understanding of the relationship between eCO_2 and IAA homeostasis.

Previous studies have extensively explored the impacts of eCO_2 on leaf photosynthesis[28–30]. A meta-analysis of 20-year rice FACE

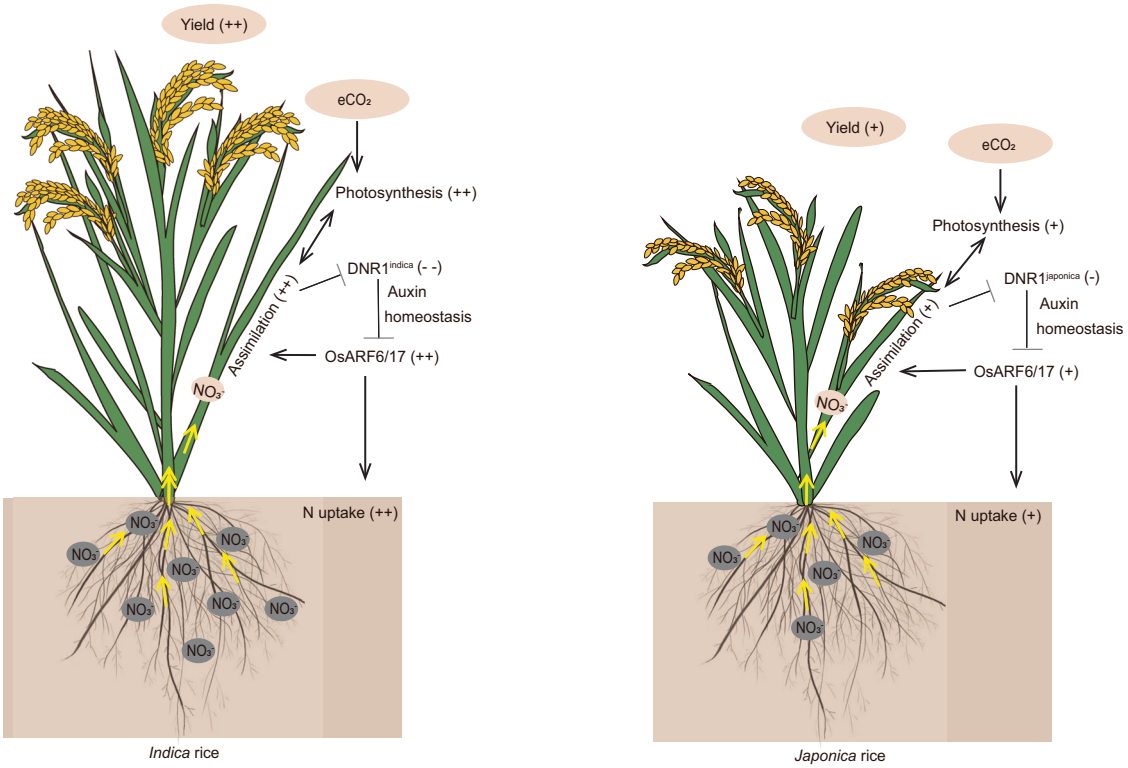

Fig. 6 | Schematic overview of the role of DNR1 in driving the divergent responses of *indica* and *japonica* rice to elevated CO_2. Rising CO_2 concentrations increase photosynthesis and rice yields by affecting a range of genes involved in uptake, transport, and assimilation of nitrate, which in turn are regulated by *DNR1*. +, ++, −, and -- indicate positive, strongly positive, negative, and strongly negative, respectively.

studies revealed that eCO_2 significantly increased the light-saturated photosynthetic rate of leaves but reduced g_s, *Vcmax*, and *Jmax* [6], consistence with our study. However, the response of photosynthetic genes to elevated CO_2 has rarely been investigated. In this study, we showed that eCO_2 promotes the abundance of photosynthetic genes (*OsPsaB*, *OsRbcs* and *OsSBPase*) more strongly in plants carrying the *indica DNR1* allele, leading to higher yield response to eCO_2. Interestingly, DNR1 mediated the regulation of photosynthetic genes expression independently of OsARFs. Further research is needed to elucidate why DNR1 influences C and N cycles through different mechanisms.

Together, our findings demonstrate that DNR1 plays a crucial role in coordinating N metabolism and C fixation to enhance plant growth in response to eCO_2. This insight provides a valuable breeding strategy for adapting to increasing atmospheric CO_2 levels by modulating DNR1, which acts as a pivotal bridge in this process. Our findings also provide insights into the relationship between N metabolism and the rate of photosynthetic C fixation in plants, particularly in the context of molecular coupling mechanisms. This study identify molecular mechanisms driving CO_2 effects among rice subspecies.

Our findings corroborate previous studies showing that in seed crops, sink capacity is a critical factor limiting yield response to eCO_2[4,31,32]. Specifically, we found that eCO_2 increased sink capacity more strongly in HJX74 than in NIL, and more strongly in *dnr1* mutants than in ZH11, resulting in higher yields (Supplementary Table 6). Similarly, eCO_2 increases the spikelet numbers per panicle more strongly in *indica* rice as compared to *japonica* rice, resulting in a heightened overall yield response[12,14]. Importantly, this sink capacity is intricately regulated by N availability. Indeed, by increasing NO_3^- use efficiency, *dnr1* stimulates sink capacity, as evidenced by increased panicle size, spikelet number, and seed size[23]. Furthermore, a previous FACE study also showed that effects of eCO_2 on rice yield are affected by N application rate[33,34]. Collectively, these results indicate that the absorption and utilization of N by rice plants is a pivotal factor influencing yield responses to eCO_2.

Two limitations of our experiment should be noted. First, we only used ZH11 as the typical *japonica* and YD6 and HJX74 as the typical *indica*. While more recipient varieties would strengthen the robustness of our results, the layout of the FACE experiment did not allow for testing more varieties. However, YD6 has been often utilized in other FACE experiments[14]. In our experiments, both YD6 and HJX74 exhibited similar responses to eCO_2 levels. Additionally, ZH11's response aligns with the average response observed in other FACE experiments involving *japonica* rice varieties[14]. These results strongly suggest that the chosen cultivars are broadly representative for *japonica* and *indica*. Second, although data from the FACE experiment have been used as a basis for hydroponic cultivation, the different environmental conditions between the two experiments may have affected rice growth and eCO_2 responses. Unfortunately, this issue is difficult to avoid. On the other hand, the results from our FACE experiment and hydroponic culture experiment consistently support the findings regarding nitrogen absorption and plant growth, suggesting that our findings are robust.

Optimizing yield response to rising atmospheric CO_2 is crucial in mitigating the anticipated supply-demand shortfall this century due to rice yield loss of climatic warming and demand increase[4,35]. Field experiments have revealed large variation in crop productivity and quality responses to eCO_2 between rice varieties, underscoring the importance of genetic variation in breeding for enhanced productivity and quality under eCO_2 conditions[4,36,37]. Our study builds on this understanding by showing that DNR1-mediated variations in NO_3^- utilization largely explains the difference in yield responses to eCO_2 between rice subspecies.

Importantly, our phylogenetic analysis of ~3000 rice accessions showed that *indica* and *japonica DNR1* alleles belong to two separate clades[23,24]. Haplotype analysis of the *DNR1* gene of these varieties

revealed four distinct haplotypes (Hap. I-IV). Notably, 98.1% of the *indica* subpopulation belongs to Hap. I, while 75.7% and 22.2% of the *japonica* subpopulation belongs to Hap. II and Hap. III, respectively[24], demonstrating consistent differentiation across existing varieties. This divergence may be attributed to high-fertilizer breeding conditions that have led to the effective utilization of the indica-type *DNR1*, while it remains underutilized in *japonica* rice. Together, these results suggest that the CO_2 fertilization effect for the vast majority *japonica* varieties can be increased by manipulating DNR1.

As *japonica* rice accounts for ~15% of global rice production[38], breeding efforts focused on NUE increase are key. Other breeding approaches may also show potential. For instance, eCO_2 increased yield by up to 30.3% in a low-yielding old *japonica* variety, suggesting that other loci are also important in determining the rice response to elevated CO_2. Together these results underscore the importance of rice varieties and agronomic practices with high NUE to improve food security as atmospheric CO_2 concentrations continue to increase.

Methods

Field experiment

FACE system. In 2021, we established a Free Air CO_2 Enrichment (FACE) system in Baolin village (31.9°N, 119.5°E), Yanling Town, Danyang City, Jiangsu Province, China. The FACE system comprises six octagonal rings, each 8 m in diameter. Three rings were designated for ambient atmospheric CO_2 concentration treatment (aCO_2), and three for elevated atmospheric CO_2 treatment (eCO_2). To prevent crossover effects, a minimum distance of 25 m was maintained between any aCO_2 and eCO_2 rings. At the center of each ring, a monitoring system was installed to track CO_2 concentration, air temperature, and wind speed. Within each eCO_2 ring, eight CO_2 sensors (VC2008T, SenseAir, Sweden) were placed above the rice canopy, evenly distributed within a 4-m circle at the ring's center.

In line with IPCC[1] predictions, atmospheric CO_2 concentrations are expected to reach between 500 (SSP5) and 800 ppm (SSP3) by 2100. Hence, we set eCO_2 treatments to mimic end-of-century conditions at ~550 ppm. PVC emission tubes, arranged to form an octagon around each eCO_2 ring at 50 cm above the rice canopy, facilitated CO_2 distribution. Considering operational costs, pure CO_2 gas was released only during the daytime (5:00 a.m. to 7:00 p.m.). This release was regulated automatically based on wind direction and speed and was halted when wind speeds exceeded 5 m s^{-1}. The average daytime CO_2 concentrations were maintained at 560 ± 19 ppm in eCO_2 treatments and 387 ± 10 ppm in aCO_2 treatments. Details of climate condition, soil properties, and FACE system can be found in Qian et al.[39].

Experimental design. To determine whether variation in the *DNR1* allele drives the divergent responses to eCO_2 between rice subspecies, we planted a typical *japonica* variety, Zhonghua 11 (ZH11), with its *dnr1* mutants, which mimics the *indica DNR1* allele in ZH11 background by reducing DNR1 abundance in 2023 and 2024. We also planted a typical *indica* variety, Hua-Jing-Xian 74 (HJX74), with a near-isogenic line (NIL) carrying the *japonica DNR1* allele in 2022 and 2023. Details of these plant materials can be found in Zhang et al.[23]. The plots for each treatment measured 1.5 m × 2 m. Two healthy rice seedlings per hill were transplanted at planting spaced at 15 cm × 25 cm intervals. N fertilizer, in the form of urea, was applied at a total rate of 180 kg N ha^{-1}. The N fertilizers were divided into three applications: 40% at soil tillage, 30% at the tillering stage, and the remaining 30% at the jointing stage. Phosphorus fertilizer, at a rate of 120 kg P_2O_5 ha^{-1}, was applied at soil tillage, while potassium fertilizer, at 160 kg K_2O ha^{-1}, was split equally between the soil tillage and jointing stages. All other agronomic practices were conducted in accordance with local agricultural recommendations.

Sampling and measurements. Light response of net photosynthesis (An) and stomatal conductance (gs) of flag leaves were measured at 11 photosynthetically active radiation (PAR) levels (in decreasing order of 1800, 1500, 1200, 1000, 800, 600, 400, 200, 100, 50 and 0 μmol m^{-2} s^{-1}) by a portable photosynthesis system (LI-6800, LI-COR, Lincoln, America) between 8:30 and 11:30 a.m. Air temperature and relative humidity in the chamber were set at 35 °C, and 60%, respectively. CO_2 concentrations were set at 400 ppm for the aCO_2 and 550 ppm for the eCO_2 treatment.

We used the rapid *A* - *Ci* response (RACiR) technique to obtain the CO_2 response of net photosynthesis rate (An) of flag leaves by a portable photosynthesis system (LI-6800, LI-COR, Lincoln, America) between 8:30 and 11:30 a.m according to Joseph et al.[40]. We set the initial and final CO_2 concentration at 50 and 1200 ppm respective, and ramp rates at 300 ppm min^{-1}. Photosynthetic active radiation, air temperature and relative humidity in the chamber were set at 1800 μmol m^{-2} s^{-1}, 35 °C, and 60%, respectively. Then, the resulting functional relationship (A-Ci curves) was used to estimate the *Vcmax* and *Jmax* FvCB model.

Chlorophyll fluorescence parameters photosystem II quantum yield (Y(II)), non-photochemical quenching (NPQ), photochemical quenching coefficient (qL), and maximum photochemical quantum yield of Photosystem II (Fv/Fm) of flag leaves were measured using the FluorPen (FluorPen FP110 - LM/D, Photon Systems Instruments, Czech) after 1-h period of darkness.

For each plot, three hills were selected to measure leaf area using a table leaf area instrument (LI-3100C, LI-COR, America). Rice plants were harvested at the heading stage and the mature stage, oven-dried at 70 °C to obtain a constant weight and then crushed. The nitrogen content was measured using an elemental analyser (vario PYRO, Elemental, German), and N uptake was calculated by multiplying the aboveground biomass by the N content. NUE is defined as grain weight divided by nitrogen supply[41].

RNA-seq analysis. Total RNAs were extracted from heading stage rice flag grown in field under the FACE system using the QIAGEN RNeasy plant mini kit (QIAGEN, 74904) following the manufacturer's instructions. Three replicate RNA-seq libraries were prepared from YD6 and ZH11 plants under aCO_2 or eCO_2, respectively. A total of the four libraries were sequenced separately using the Illumina Novaseq platform. Raw sequencing reads were cleaned by removing adaptor sequences, reads containing poly-N sequences, and low-quality reads. Approximately 44,226,120 clean reads were mapped to the Nipponbare reference genome using Hisat2 v2.0.5[42]. After data were mapped, normalization was performed and then FPKM (fragments per kilobase per million mapped reads) was calculated using RESM software[43]. As previously described[44], a false discovery rate (FDR) <0.05 and absolute value of log2 ratio≥2 were used to identify differentially expressed genes in YD6 and ZH11 samples under aCO_2 or eCO_2, respectively.

Hydroponic experiment

Plant materials. The plant materials including a pair of near isogenic materials of NIL-$DNR1^{HJX74}$ (HJX74) and NIL-$DNR1^{IRAP9}$ (NIL), as well as *pAct::DNR1-Flag* and *dnr1* under Zhonghua 11 (ZH11) background, and *pAct::OsARF6-Flag* and *pAct::OsARF17-Flag* under ZH11/*pAct::DNR1-Flag*. Details of these plant materials can be found in Zhang et al.[21] and Huang et al.[22].

Hydroponic culture. Seeds were soaked in 20% sodium hypochlorite solution for 30 min for disinfection and selected with uniform growth for further analyses as described previously[45]. The 7-day-old seedlings were transferred to PVC pots containing 10 L of nutrient solution (1.25 mM NH_4NO_3, 0.3 mM $NaH_2PO_4{\cdot}2H_2O$, 0.35 mM K_2SO_4, 1 mM $CaCl_2$, 1 mM $MgSO_4{\cdot}7H_2O$, 20 μM EDTA-Fe, 0.5 mM Na_2SiO_3, 9 μM $MnCl_2$, 20 μM H_3BO_3, 0.77 μM $ZnSO_4$, 0.32 μM $CuSO_4$, and 0.39 μM

$(NH_4)_6Mo_7O_{24}$, pH 5.5) and grown at either aCO_2 levels or eCO_2 levels for 2 weeks. All nutrient solutions were replaced twice per week, pH was adjusted to 5.5 daily. The average daytime (8:00 a.m. to 8:00 p.m.) CO_2 concentrations were maintained at 598 ± 32 ppm in eCO_2 treatments and 408 ± 28 ppm in aCO_2 treatments. The mean day/night air temperature was maintained at 30 °C/25 °C with 60% relative humidity. The LED lamps were positioned 50 cm above the rice, providing a mean photon flux of 500 μmol m^{-2} s^{-1} during the daytime.

^{15}N uptake analysis. After growth in hydroponic condition (1.25 mM NH_4NO_3) for 2 weeks, rice root $^{15}NH_4^+$ and $^{15}NO_3^-$ influx measurements were performed as described elsewhere[44,46]. Specifically, 14-day-old rice plants were transferred first to 0.1 mM $CaSO_4$ for 1 min, then to a complete nutrient solution containing 2.5 mM $K^{15}NO_3$ (Sigma, 335134, 98% atom excess ^{15}N) or 1.25 mM $(^{15}NH_4)_2SO_4$ (Aladdin, A110168, 99% atom excess ^{15}N) instead of 1.25 mM NH_4NO_3 as the N source for 5 min. The plants were incubated in 0.1 mM CaSO4 for 1 min before the roots were collected and dried at 80 °C for 72 h. Root dry weight was recorded and the 15 N content was measured using the IsoPrime100 elemental analyser (Elementar, Germany). Finally, influx of $^{15}NH_4^+$ and $^{15}NO_3^-$ was calculated as described elsewhere[24].

Root system analysis. Roots from rice plants grown in the aCO_2 and eCO_2 treatments for 14 d were cut off and spread out in water in a transparent dish. Subsequently, the root system was scanned as described previously[24].

Measurement of NR activity. Fresh plant material (~1 g) from individual rice plant grown at either aCO_2 levels or eCO_2 levels for 2 weeks was used to measure NR activity, following the instruction manual of the NR Kit (Solarbio LIFE SCIENCES, BC0080).

Quantitative real time PCR (RT-qPCR) analysis. After growth in hydroponic condition (1.25 mM NH_4NO_3) for 2 weeks, total RNAs were extracted from different plant tissues using the TRIzol reagent (Ambion), and full-length cDNAs were reverse transcribed using a cDNA synthesis kit (Accurate Biology, AG11728). Subsequent RT-qPCR was performed according to the manufacturer's instructions (Accurate Biology, AG11718). Each RT-qPCR assay included at least three biological replicates. As for time course experiment, selected eight time points (0, 15 min, 30 min, 2 h, 24 h, 72 h, 7 d, 14 d) for sample preparation and extracted RNA for RT-qPCR. The rice *ACTIN1* gene was used as an internal reference. Relevant RT-qPCR primer sequences are listed in Supplementary Table 4.

ChIP-qPCR assays. The ChIP-qPCR protocol has been previously described[23]. Approximately 2 g of two-week-old *pAct::OsARF6-Flag* and *pAct::OsARF17-Flag* overexpression lines in the Wuyunjing 7 (WYJ7) background, grown under aCO_2 and eCO_2 conditions, were cross-linked with 1% formaldehyde under vacuum for 15 min to stabilize protein-DNA interactions. The samples were then ground to a fine powder in liquid N. Nuclei were isolated and lysed, and chromatin was fragmented by sonication into ~500 bp fragments. The chromatin was incubated overnight at 4 °C with 7 μg of anti-Flag antibody (Sigma, F1804) for immunoprecipitation. The following day, the samples were washed, eluted, and reverse-cross-linked, followed by DNA purification. Enrichment of specific DNA fragments was analyzed by RT-qPCR using three biological replicates. Relevant qPCR primer sequences are provided in Supplementary Table 7.

Western blotting. Total protein was extracted in 50 mM Tris-HCl (pH 7.5), 150 mM NaCl, 0.1% NP-40 detergent, 10% Glycerol, 1 mM DTT with added protease inhibitor cocktail (Roche LifeScience) and transferred onto a nitrocellulose membrane. Then, after blocking with 5% milk solution for 1 h, the nitrocellulose membrane was incubated with antibodies. The DNR1 protein was detected by probing the membrane with anti-DNR1 (ABclonal) and proteins involved in photosynthesis were detected by anti-PsbA (Agrisera, AS05084), anti-PsaB (Agrisera, AS10695), anti-RbcS (Agrisera, AS07259), anti-RbcL (Agrisera, AS03037) and anti-SBPase (Agrisera, AS152873), respectively. The result of immunoblotting was visualized on the Tanon-5200 Chemiluminescent Imaging System and grayscale analysis was used Tanon image GIS Semi-quantitative analysis (Tanon Science and Technology).

In vitro transient transactivation assays. As described elsewhere[23], the *indica* variety YD6 was planted under different CO_2 treatments for 10 days. Firstly, the free IAA content of YD6 under two conditions was detected and then extracted rice protoplasts, subsequently, used the effector plasmids *pRTBD-OsARF6* and *pRTBD-OsARF17* to drive the reporters *5×GAL4-OsNRT1.1B, -OsNRT2.3a, -OsNPF2.4, -OsNIA2, -OsPsbA2, -OsPsaB2, -OsRbcs2, OsRbcs4, OsRbcL* and *OsSBPase*, respectively. Transient transactivation assays were performed as described elsewhere[47]. The Dual-Luciferase Reporter Assay System (Promega, E1960) was used to perform the luciferase activity assays, with the Renilla LUC gene as an internal control. Relevant PCR primer sequences are listed in Supplementary Table 8.

Determination of free IAA content. Root tip samples (~50 mg) were ground into a powder in liquid N and extracted with methanol/water/formic acid (15:4:1, V/V/V). The combined extracts were evaporated to dryness under a N gas stream, reconstituted in 80% methanol (V/V), and filtered through a PTFE membrane (0.22 μm, Anpel). The final solution was then analyzed using an LC-ESI-MS/MS system and an ESI-triple quadrupole-linear ion trap (QTRAP)-MS system (Wuhan Triploid Biotech).

Statistical analysis

We analyzed the data in the field and hydroponic experiments through two-sided Student's *t* tests and two-way ANOVA, including CO_2 and variety as fixed effects. When the ANOVA indicated interactive effects, multiple comparisons were performed using the least significant difference test at the significance level of $P = 0.05$. All analyses were performed with the statistical package SPSS 27.

Reporting summary

Further information on research design is available in the Nature Portfolio Reporting Summary linked to this article.

Data availability

Raw RNA-seq data were deposited at the National Genomics Data Center, Genome Sequence Archive (GSA) (accession number PRJCA024327 [https://ngdc.cncb.ac.cn/gsa/s/Hz4L1U30]). Source data are provided with this paper.

References

1. IPCC. *Working Group 1 Contribution to the Sixth Assessment Report of the Intergovernmental Panel on Climate Change. Climate Change 2021: The Physical Science Basis* (Cambridge University Press, Cambridge, USA, 2021).
2. National Aeronautics and Space Administration (NASA), 2024. https://climate.nasa.gov/vital-signs/carbon-dioxide/.
3. Wang, S. et al. Recent global decline of CO_2 fertilization effects on vegetation photosynthesis. *Science* **370**, 1295–1300 (2020).
4. Ainsworth, E. A. & Long, S. P. 30 years of free-air carbon dioxide enrichment (FACE): What have we learned about future crop productivity and its potential for adaptation? *Glob. Chang Biol.* **27**, 27–49 (2021).
5. Rezaei, E. E. et al. Climate change impacts on crop yields. *Nat. Rev. Earth Environ.* **4**, 831–846 (2023).

6. Hu, S. et al. Response of rice growth and leaf physiology to elevated CO_2 concentrations: a meta-analysis of 20-year FACE studies. *Sci. Total Environ.* **807**, 151017 (2022).
7. Fahad, S. et al. Major constraints for global rice production. in *Advances in Rice Research for Abiotic Stress Tolerance,* 1–22 (Elsevier, 2019).
8. Wang, X. et al. Emergent constraint on crop yield response to warmer temperature from field experiments. *Nat. Sustain.* **3**, 908–916 (2020).
9. Zhu, P. Warming reduces global agricultural production by decreasing cropping frequency and yields. *Nat. Clim. Change* **12**, 1–8 (2022).
10. Jing, C. et al. Multiple domestications of Asian rice. *Nat. Plants* **9**, 1221–1235 (2023).
11. Purugganan, M. D. & Fuller, D. Q. The nature of selection during plant domestication. *Nature* **457**, 843–848 (2009).
12. Hu, S., Wang, Y. & Yang, L. Response of rice yield traits to elevated atmospheric CO_2 concentration and its interaction with cultivar, nitrogen application rate and temperature: a meta-analysis of 20 years FACE studies. *Sci. Total Environ.* **764**, 142797 (2021).
13. Wang, W. et al. Elevated CO_2-induced changes in cytokinin and nitrogen metabolism are associated with different responses in the panicle architecture of two contrasting rice genotypes. *Plant Growth Regul.* **89**, 119–129 (2019).
14. Lv, C. et al. Response of rice yield and yield components to elevated [CO_2]: a synthesis of updated data from FACE experiments. *Eur. J. Agron.* **112**, 125961 (2020).
15. Bloom, A. J., Burger, M., Asensio, J. S. R. & Cousins, A. B. Carbon dioxide enrichment inhibits nitrate assimilation in wheat and *arabidopsis*. *Science* **328**, 899–903 (2010).
16. Terrer, C. et al. Nitrogen and phosphorus constrain the CO_2 fertilization of global plant biomass. *Nat. Clim. Change* **9**, 684–689 (2019).
17. Wang, Y. Y., Cheng, Y. H., Chen, K. E. & Tsay, Y. F. Nitrate transport, signaling, and use efficiency. *Annu. Rev. Plant Biol.* **69**, 85–122 (2018).
18. Li, Y., Fan, X. & Shen, Q. The relationship between rhizosphere nitrification and nitrogen-use efficiency in rice plants. *Plant Cell Environ.* **31**, 73–85 (2008).
19. Hu, B. et al. Variation in *NRT1.1B* contributes to nitrate-use divergence between rice subspecies. *Nat. Genet.* **47**, 834–838 (2015).
20. Zhang, Z. & Chu, C. Nitrogen-use divergence between *indica* and *japonica* rice: variation at nitrate assimilation. *Mol. Plant* **13**, 6–7 (2020).
21. Gao, Z. et al. The *indica* nitrate reductase gene *OsNR2* allele enhances rice yield potential and nitrogen use efficiency. *Nat. Commun.* **10**, 5207 (2019).
22. Gao, Y. et al. MYB61 is regulated by GRF4 and promotes nitrogen utilization and biomass production in rice. *Nat. Commun.* **11**, 5219 (2020).
23. Zhang, S. et al. Natural allelic variation in a modulator of auxin homeostasis improves grain yield and nitrogen use efficiency in rice. *Plant Cell* **33**, 566–580 (2021).
24. Huang, Y. et al. Improving rice nitrogen-use efficiency by modulating a novel monouniquitination machinery for optimal root plasticity response to nitrogen. *Nat. Plants* **9**, 1902–1914 (2023).
25. Li, C. R. et al. Responses of carboxylating enzymes, sucrose metabolizing enzymes and plant hormones in a tropical epiphytic CAM orchid to CO_2 enrichment. *Plant Cell Environ.* **25**, 369–377 (2002).
26. Teng, N. J. et al. Elevated CO_2 induces physiological, biochemical and structural changes in leaves of Arabidopsis thaliana. *New Phytol.* **172**, 92–103 (2006).
27. Li, X. M. et al. Influence of elevated CO_2 and O_3 on IAA, IAA oxidase and peroxidase in the leaves of ginkgo trees. *Biol. Plant* **53**, 339–342 (2009).
28. Bernacchi, C. J. et al. Photosynthesis and stomatal conductance responses of poplars to free-air CO_2 enrichment (PopFACE) during the first growth cycle and immediately following coppice. *New Phytol.* **159**, 609–621 (2003).
29. Long, S. P. et al. Rising atmospheric carbon dioxide: plants FACE the future. *Annu. Rev. Plant Biol.* **55**, 591–628 (2004).
30. Cai, C. et al. Do all leaf photosynthesis parameters of rice acclimate to elevated CO_2, elevated temperature, and their combination, in FACE environments? *Glob. Change Biol.* **24**, 1685–1707 (2018).
31. Nakano, H. et al. Quantitative trait loci for large sink capacity enhance rice grain yield under free-air CO_2 enrichment conditions. *Sci. Rep.* **7**, 1827 (2017).
32. Takai, T. et al. *MORE PANICLES 3*, a natural allele of *OsTB1/FC1*, impacts rice yield in paddy fields at elevated CO_2 levels. *Plant J.* **114**, 729–742 (2023).
33. Kim, H. Y. et al. Growth and nitrogen uptake of CO_2-enriched rice under field conditions. *New Phytol.* **150**, 223–229 (2001).
34. Kim, H. et al. Seasonal changes in the effects of elevated CO_2 on rice at three levels of nitrogen supply: a free air CO_2 enrichment (FACE) experiment. *Glob. Change Biol.* **9**, 826–837 (2003).
35. Ray, D. K. et al. Yield trends are insufficient to double global crop production by 2050. *PLoS ONE* **8**, e66428 (2013).
36. Ziska, L. H. et al. Food security and climate change: on the potential to adapt global crop production by active selection to rising atmospheric carbon dioxide. *Proc. R. Soc. B.* **279**, 4097–4105 (2012).
37. Zhu, C. et al. Carbon dioxide (CO_2) levels this century will alter the protein, micronutrients, and vitamin content of rice grains with potential health consequences for the poorest rice-dependent countries. *Sci. Adv.* **4**, eaaq1012 (2018).
38. Koizumi, T. & Furuhashi, G. Global rice market projections distinguishing japonica and indica rice under climate change. *Jpn Agric. Res. Q.* **50**, 63–91 (2020).
39. Qian, H. et al. Intermittent flooding lowers the impact of elevated atmospheric CO_2 on CH_4 emissions from rice paddies. *Agric. Ecosyst. Environ.* **329**, 107872 (2022).
40. Stinziano, J. R. et al. The rapid A-Ci response: photosynthesis in the phenomic era. *Plant Cell Environ.* **40**, 1256–1262 (2017).
41. Good, A. G., Shrawat, A. K. & Muench, D. G. Can less yield more? Is reducing nutrient input into the environment compatible with maintaining crop production? *Trends Plant Sci.* **9**, 597–605 (2004).
42. Kim, D. et al. Graph-based genome alignment and genotyping with HISAT2 and HISAT-genotype. *Nat. Biotechnol.* **37**, 907–915 (2019).
43. Li, B. & Dewey, C. N. RSEM: accurate transcript quantification from RNA-Seq data with or without a reference genome. *BMC Bioinform.* **12**, 323 (2011).
44. Benjamini, Y. et al. Controlling the false discovery rate in behavior genetics research. *Behav. Brain Res.* **125**, 279–284 (2001).
45. Ho, C., Lin, S. H., Hu, H. & Tsay, Y. F. CHL1 functions as a nitrate sensor in plants. *Cell* **138**, 1184–1194 (2009).
46. Li, S. et al. Modulating plant growth-metabolism coordination for sustainable agriculture. *Nature* **560**, 595–600 (2018).
47. Wang, S. et al. The *OsSPL16-GW7* regulatory module determines grain shape and simultaneously improves rice yield and grain quality. *Nat. Genet.* **47**, 949–954 (2015).

Acknowledgements

We thank Dr. Chunwu Zhu for valuable comments. This work was supported by the National Natural Science Foundation of China (32122065 to S.L., 32271635 to Y.J., 32372121 and 32441056 to S.L., 32301354 to H.Q. and 32401866 to S.Z.), the Natural Science Foundation of Jiangsu Province (BK20230979 to H.Q. and BK20241559 to S.Z.), Jiangsu Carbon

Peak Carbon Neutrality Science and Technology Innovation Fund project (BE2022308 to Y.D.), and the China Postdoctoral Science Foundation (GZB20240320 to S.Z.).

Author contributions

Y.J. and S.L. designed the study. Y.L., H.Q., and Y.W. conducted the field experiment. S.Z., C.S., and Y.L. conducted the hydroponic experiment. Y.J., S.L., Y.D., Y.L., and S.Z. drafted the paper. Shuijun Hu, W.Z., Shan Huang, S.W., Z.L., G.L., X.F., and K.J.v.G. reviewed and commented on the manuscript.

Competing interests

The authors declare no competing interests.

Additional information

Supplementary information The online version contains supplementary material available at https://doi.org/10.1038/s41467-024-55809-3.

Correspondence and requests for materials should be addressed to Yanfeng Ding, Shan Li or Yu Jiang.

Peer review information *Nature Communications* thanks Chengcai Chu, Brent Kaiser and the other, anonymous, reviewer(s) for their contribution to the peer review of this work. A peer review file is available.